

Freeze-in sterile neutrino dark matter in feeble gauged $B - L$ model

Osamu Seto,^{1,*} Takashi Shimomura,^{2,†} and Yoshiki Uchida^{3,4,‡}

¹*Department of Physics, Hokkaido University, Sapporo 060-0810, Japan*

²*Faculty of Education, Miyazaki University, Miyazaki 889-2192, Japan*

³*Key Laboratory of Atomic and Subatomic Structure and Quantum Control (MOE),*

Guangdong Basic Research Center of Excellence for Structure and

Fundamental Interactions of Matter, Institute of Quantum Matter,

South China Normal University, Guangzhou 510006, China

⁴*Guangdong-Hong Kong Joint Laboratory of Quantum Matter,*

Guangdong Provincial Key Laboratory of Nuclear Science,

Southern Nuclear Science Computing Center,

South China Normal University, Guangzhou 510006, China

Abstract

We consider the gauged $U(1)_{B-L}$ model and examine the situation where the sterile neutrino is a dark matter candidate produced by the freeze-in mechanism. In our model, the dark matter N is mainly produced by the decay of a $U(1)_{B-L}$ breaking scalar field ϕ . We point out that the on-shell production of ϕ through annihilation of the $U(1)_{B-L}$ gauge field Z' plays an important role. We find that the single production of Z' from the photon bath is one of the main production processes of Z' . To prevent N from being overproduced, we show that the $U(1)_{B-L}$ gauge coupling constant g_{B-L} must be as small as 10^{-13} – 10^{-10} . We also consider the case where the decay of ϕ into N is kinematically forbidden. In this case, N is generated by the scattering of Z' and the g_{B-L} takes values of 10^{-7} – 10^{-6} , which can be explored in collider experiments like FASER.

*Electronic address: seto@particle.sci.hokudai.ac.jp

†Electronic address: shimomura@cc.miyazaki-u.ac.jp

‡Electronic address: uchida.yoshiki@m.scnu.edu.cn

I. INTRODUCTION

Nonvanishing masses of neutrinos indicate the existence of the standard model (SM) gauge singlet right-handed (RH) neutrinos. Such a RH neutrino would be referred to as sterile neutrino because those do not interact through the weak interaction, except through possible tiny mixing with left-handed (LH) active neutrinos. Massive sterile neutrinos are electrically neutral and could be very long lived if the mixing with active neutrinos, in other words Yukawa couplings, is small enough. Then one of the RH neutrinos is a good candidate for dark matter (DM) in our Universe [1–4] (for a review see e.g., Refs. [5, 6]), while the others can generate neutrino masses through so-called seesaw mechanism [7–10].

In the minimal scenario of sterile neutrino DM N , sterile neutrinos never reach at thermal equilibrium but are thermally produced as warm DM, by so-called Dodelson-Widrow mechanism, through the mixing with active neutrinos [1]. However such sterile neutrino DM have been confronted with astrophysical x-ray bounds and Lyman- α constraints on its free streaming scale [11–15]¹. We may seek another production mechanism in an extended model of the SM where an additional interaction besides the mixing exists. While RH neutrinos are singlet under the SM, they might be charged under an additional gauge symmetry. Gauged $B - L$ (Baryon number – Lepton number) symmetry is a theoretically well motivated extension of the SM [18–20]. Since a RH neutrino carries lepton number, sterile neutrinos are charged under the $U(1)_{B-L}$. Production of sterile neutrinos through the $U(1)_{B-L}$ gauge boson Z' is a viable alternative [21] in the minimal $U(1)_{B-L}$ model where one scalar to break the $B - L$ gauge symmetry and three RH neutrinos to cancel all anomalies are minimally introduced. Then, if the $B - L$ gauge coupling constant g_{B-L} is of the order of unity, sterile neutrinos would be easily thermalized by the new $U(1)_{B-L}$ gauge interaction, which would give rise to overabundant or too warm, unless the cosmic thermal history is non-standard [21] or parity-odd sterile neutrino [22] is as heavy as weakly interacting massive particle [23].

On the other hand, for the very small g_{B-L} , sterile neutrino DM is generated non-thermally by the scattering or decay in the thermal plasma. Such non-thermal production had been applied for various particles [24, 25], which was coined as “freeze-in” produc-

¹ The production by the mixing is available in the case that the production rate is enhanced by the resonance effect under a large lepton asymmetric background [16]. See, for a recent study on cosmological constraints on large lepton asymmetry, e.g., Ref. [17].

tion [26]. Processes involving Z' [27–33] appear to be enough to explain the production of sterile neutrino DM. However, the $U(1)_{B-L}$ breaking scalar ϕ contributions in addition to Z' cannot be ignored and was shown to be important for qualitatively and theoretical consistency [34], because the production processes occur most efficiently at a low temperature and are described by the broken gauge theory. In Ref. [34], the processes involving ϕ have been fully formulated, nevertheless effects of ϕ have not completely evaluated for $m_\phi > 2m_N$ and $m_{Z'} < 2m_N$ because the decay width of ϕ is too narrow in numerical calculations. We note that calculation for the $m_{Z'} > 2m_N$ case in Ref. [34] is valid.

In this paper, to take the scalar contributions into account appropriately for $m_{Z'} < 2m_N$, we solve the set of Boltzmann equations of not only sterile neutrino and the Z' but also the ϕ with and without the mixing with the SM Higgs boson. As the decay and its inverse decay of Z' are dominant processes for production or thermalization of Z' [34], we point out that this is the case for ϕ as well. We also point out that the single Z' production modes are significant in the Z' production. We find that the required g_{B-L} must be smaller than $\mathcal{O}(10^{-10})$ to reproduce the observed DM abundance for $m_\phi > 2m_N$. On the other hand, for $m_\phi < 2m_N$, the cosmological interesting parameter region, $g_{B-L} \lesssim 10^{-6}$, can be probed by long lived Z' searches as have been reported in the literature [27, 31, 34, 35].

This paper is organized as follows. We give Lagrangian of the model and the decay rate of singlet-like scalar ϕ in Sec. II, and summarize Boltzmann equations to be solved in Sec. III. In Sec. IV, we show our results for $m_\phi > 2m_N$ with emphasizing the contribution of ϕ to DM abundance. For this parameter range to reproduce the correct DM abundance, all of N , Z' and ϕ are feeble particles and never reach thermal equilibrium. We solve the evolution of the number densities of such multiple species in the feeble $U(1)_{B-L}$ sector. We also discuss cosmological, astrophysical and experimental constraints and implications for the opposite mass spectrum case of $m_\phi < 2m_N$. We conclude this paper in Sec. V.

II. MODEL

We consider the minimal gauged $U(1)_{B-L}$ model studied in Ref. [34]. In this model, three generations of RH neutrinos (ν_R^i , $i = 1, 2, 3$) are introduced to cancel the gauge anomalies. One complex scalar Φ , which spontaneously breaks the $B - L$ gauge symmetry, is also introduced as the origin of Majorana mass of RH neutrinos. The gauge charge assignment is

	Q^i	u^i	d^i	L^i	e_R^i	ν_R^i	H	Φ
$SU(3)_C$	3	3	3	1	1	1	1	1
$SU(2)_L$	2	1	1	2	1	1	2	1
$U(1)_Y$	$\frac{1}{6}$	$\frac{2}{3}$	$-\frac{1}{3}$	$-\frac{1}{2}$	-1	0	$\frac{1}{2}$	0
$U(1)_{B-L}$	$\frac{1}{3}$	$\frac{1}{3}$	$\frac{1}{3}$	-1	-1	-1	0	2

TABLE I: Particle content and gauge charge assignment. The RH neutrinos are denoted as ν_R^i ($i = 1, 2, 3$) and new scalar boson is denoted as Φ .

shown in Table I. Here, Q (u_R, d_R) and L (e_R, ν_R) denote the LH (RH) quarks and leptons, respectively, and the SM Higgs doublet is denoted by H .

A. Lagrangian

The Lagrangian of the model is

$$\mathcal{L} = \mathcal{L}_{\text{SM}} + \mathcal{L}_{\nu_R} + \mathcal{L}_{\text{gauge}} + |D_\mu \Phi|^2 - V, \quad (1)$$

where \mathcal{L}_{SM} represents the SM Lagrangian without a scalar potential. The Lagrangian regarding the RH neutrino \mathcal{L}_{ν_R} is given by

$$\mathcal{L}_{\nu_R} = \frac{1}{2} \overline{\nu_R^i} (i \not{D}) \nu_R^i - y_{\nu_{ij}} \overline{L^i} \tilde{H} \nu_R^j - \frac{1}{2} y_{\nu_{Ri}} \Phi \overline{\nu_R^i}^C \nu_R^i + \text{H.c.}, \quad (2)$$

where the superscript C denotes the charge conjugation, and $\tilde{H} \equiv \epsilon H^\dagger$ is the complex conjugate Higgs field with ϵ being the antisymmetric tensor of $SU(2)_L$. The Yukawa couplings for the LH lepton doublets and RH neutrinos are denoted by $y_{\nu_{ij}}$ and $y_{\nu_{Ri}}$, respectively, in which i and j are indices of flavor or generation. Without loss of generality, we can work on the diagonal basis of $y_{\nu_{Ri}}$.

The covariant derivative in this model is given as

$$D_\mu = \partial_\mu - ig_2 W_\mu - ig_1 Y B_\mu - ig_{B-L} Q_{B-L} X_\mu, \quad (3)$$

where W_μ , B_μ and X_μ represent the gauge fields of $SU(2)_L$, $U(1)_Y$, and $U(1)_{B-L}$, and g_2 , g_1 , and g_{B-L} are the corresponding gauge coupling constants, respectively. The $U(1)_Y$ and $U(1)_{B-L}$ charges are denoted as Y and Q_{B-L} , which are shown in Table I. We omit the $SU(3)_C$ color interaction because it is irrelevant with our discussion.

The Lagrangian for the $B - L$ gauge boson kinetic term, $\mathcal{L}_{\text{gauge}}$, consists of

$$\mathcal{L}_{\text{gauge}} = -\frac{1}{4}X_{\mu\nu}X^{\mu\nu} + \frac{\varepsilon}{2}B_{\mu\nu}X^{\mu\nu}, \quad (4)$$

where $X_{\mu\nu}$ and $B_{\mu\nu}$ represent the gauge field strength of X and B , respectively. The second term is the gauge kinetic mixing term with a mixing parameter ε . For the sake of minimality, we set the kinetic mixing parameter to be negligibly small and omit this term throughout this paper².

The fourth term of Eq. (1) is the kinetic term of Φ , and the last one V is the scalar potential which is given by

$$V = \frac{\lambda_1}{2} \left(|H|^2 - \frac{v^2}{2} \right)^2 + \frac{\lambda_2}{2} \left(|\Phi|^2 - \frac{v_{B-L}^2}{2} \right)^2 + \lambda_3 \left(|H|^2 - \frac{v^2}{2} \right) \left(|\Phi|^2 - \frac{v_{B-L}^2}{2} \right), \quad (5)$$

where $\lambda_1, \lambda_2, \lambda_3$ are real and positive parameters. On the electroweak and $B - L$ broken vacuum, the scalar bosons are expanded around its vacuum expectation value (vev), v and v_{B-L} , respectively as

$$H = \begin{pmatrix} 0 \\ \frac{1}{\sqrt{2}}(v + \phi_H) \end{pmatrix}, \quad \Phi = \frac{1}{\sqrt{2}}(v_{B-L} + \phi_{B-L}), \quad (6)$$

where ϕ_H and ϕ_{B-L} are the dynamical degree of freedom. Here, the Nambu-Goldstone bosons to be absorbed by the gauge bosons are omitted.

After the spontaneous symmetry breaking of $SU(2)_L \times U(1)_Y$ and $U(1)_{B-L}$ symmetries, the gauge bosons and RH neutrinos acquire the masses. The neutrinos also acquire the masses via the type-I seesaw mechanism. We denote the mass eigenstates of the active, sterile neutrinos as ν, N_i , and also those of the extra gauge and scalar bosons as Z' and h, ϕ , respectively. The masses of N_i and Z' are given by

$$m_{N_i} \simeq \frac{y_{\nu R i}}{\sqrt{2}} v_{B-L}, \quad (7)$$

$$m_{Z'} = 2g_{B-L} v_{B-L}, \quad (8)$$

where we assume that v_{B-L} is much larger than v . Using Eqs. (7) and (8), the Majorana Yukawa coupling and vev are expressed by the N_i and Z' mass, respectively, in the following

² The kinetic mixing can be generated through loop processes. Such a loop-induced kinetic mixing is not finite and should be renormalized. We assume that our kinetic mixing parameter is tiny after the loop induced ones are renormalized.

section. The masses of h and ϕ are given by

$$m_h^2 = \frac{1}{2} \left(\lambda_1 v^2 + \lambda_2 v_{B-L}^2 + \frac{\lambda_1 v^2 - \lambda_2 v_{B-L}^2}{\cos(2\alpha)} \right), \quad (9)$$

$$m_\phi^2 = \frac{1}{2} \left(\lambda_1 v^2 + \lambda_2 v_{B-L}^2 - \frac{\lambda_1 v^2 - \lambda_2 v_{B-L}^2}{\cos(2\alpha)} \right), \quad (10)$$

where α is the scalar mixing angle defined by

$$\sin(2\alpha) \simeq \frac{vm_{Z'}}{m_\phi^2 - m_h^2} \frac{\lambda_3}{g_{B-L}}. \quad (11)$$

The mass eigenstates, h and ϕ , are related with ϕ_H and ϕ_{B-L} as

$$\begin{pmatrix} \phi_H \\ \phi_{B-L} \end{pmatrix} = \begin{pmatrix} \cos \alpha & \sin \alpha \\ -\sin \alpha & \cos \alpha \end{pmatrix} \begin{pmatrix} h \\ \phi \end{pmatrix}. \quad (12)$$

For the rest of this paper, we identify h as the SM Higgs boson with the mass of 125 GeV.

B. Decay rates of ϕ

In our previous work [34], the freeze-in productions of N from nonthermal decays and/or scatterings of Z' were studied by solving the Boltzmann equations. Here and hereafter, the DM is denoted as N , which is sequestered from the SM particles, one among the three sterile neutrinos. The other N_i responsible to generate neutrino mass are denoted by ν_R . The relevant decay rates and cross sections of N and Z' can be found in Ref. [34]. In this subsection, we present the decay rates including ϕ and h which are newly studied in this paper.

One of the relevant interaction Lagrangians is the gauge interaction with Z' given by

$$\mathcal{L}_{\text{gauge}} = 2g_{B-L}m_{Z'} \cos \alpha Z'_\mu Z'^\mu \phi + 4g_{B-L}^2 \cos^2 \alpha Z'_\mu Z'^\mu \phi^2, \quad (13)$$

and the other one is the Yukawa interactions given by

$$\mathcal{L}_{\text{yukawa}} = -\frac{\sqrt{2}m_f}{v} \sin \alpha \bar{f} f \phi - g_{B-L} \frac{\sqrt{2}m_N}{m_{Z'}} \cos \alpha \overline{N_i^C} N_i \phi, \quad (14)$$

where the Yukawa coupling of a fermion f is replaced by its mass m_f and v . The partial

decay rates of $\phi \rightarrow Z'Z'$ and NN , $f\bar{f}$ are given by

$$\Gamma(\phi \rightarrow Z'Z') = (g_{B-L} \cos \alpha)^2 \frac{m_\phi}{4\pi} \sqrt{1 - \frac{4m_{Z'}^2}{m_\phi^2} \frac{m_\phi^2 - 4m_{Z'}^2 + 12\frac{m_{Z'}^4}{m_\phi^2}}{m_{Z'}^2}}, \quad (15a)$$

$$\Gamma(\phi \rightarrow N_i N_i) = (g_{B-L} \cos \alpha)^2 \frac{m_\phi}{4\pi} \sum_i \left(\frac{m_{N_i}}{m_{Z'}} \right)^2 \left(1 - \frac{4m_{N_i}^2}{m_\phi^2} \right)^{3/2}, \quad (15b)$$

$$\Gamma(\phi \rightarrow f\bar{f}) = \sin^2 \alpha \frac{m_\phi}{4\pi} \left(\frac{m_f}{v} \right)^2 \left(1 - \frac{4m_f^2}{m_\phi^2} \right)^{3/2}. \quad (15c)$$

The scalar boson ϕ also can decay into the SM Higgs bosons, $\phi \rightarrow hh$. However, we consider the case where ϕ is lighter than h , and therefore such production is kinematically forbidden. On the other hand, the decay of h into $\phi\phi$ is possible and its decay rate is given by

$$\Gamma_h(h \rightarrow \phi\phi) = \frac{\sqrt{m_h^2 - 4m_\phi^2}}{16\pi m_h^2} |C_{h\phi\phi}|^2, \quad (16)$$

with

$$C_{h\phi\phi} = \frac{\sin(2\alpha)(m_h^2 + 2m_\phi^2)(m_{Z'} \sin \alpha - 2g_{B-L} v \cos \alpha)}{2vm_{Z'}}. \quad (17)$$

III. THE BOLTZMANN EQUATION

In this section, we show the Boltzmann equations of N , Z' and ϕ for freeze-in production. The Boltzmann equations for the number density of N , Z' and ϕ are given by

$$\frac{dn_N}{dt} + 3Hn_N = \sum_{i,j=f,Z'} \langle \sigma v(ij \rightarrow NN) \rangle (n_i n_j - n_N^2) + \sum_{i=Z',\phi,h} \langle \Gamma(i \rightarrow NN) \rangle n_i, \quad (18a)$$

$$\begin{aligned} \frac{dn_{Z'}}{dt} + 3Hn_{Z'} &= \sum_{i,j=f} \langle \sigma v(ij \rightarrow Z'Z') \rangle (n_i n_j - n_{Z'}^2) + \sum_{i=\phi,h} \langle \Gamma(i \rightarrow Z'Z') \rangle n_i \\ &\quad - \sum_{i=\phi,h} \langle \sigma v(Z'Z' \rightarrow i) \rangle n_{Z'}^2 + \sum_{i,j,k=f,\gamma} \langle \sigma v(Z'i \rightarrow jk) \rangle n_i (n_{Z'} - n_{Z'}^{\text{eq}}) \\ &\quad - \sum_{i,j=f} \langle \Gamma(Z' \rightarrow ij) \rangle (n_{Z'} - n_{Z'}^{\text{eq}}), \end{aligned} \quad (18b)$$

$$\begin{aligned} \frac{dn_\phi}{dt} + 3Hn_\phi &= \sum_{i,j=f} \langle \sigma v(ij \rightarrow \phi\phi) \rangle (n_i n_j - n_\phi^2) \\ &\quad + \langle \sigma v(Z'Z' \rightarrow \phi) \rangle n_{Z'}^2 - \langle \Gamma(\phi \rightarrow Z'Z') \rangle n_\phi - \sum_{i,j=f} \langle \Gamma(\phi \rightarrow ij) \rangle (n_\phi - n_\phi^{\text{eq}}), \end{aligned} \quad (18c)$$

where i, j , and k are possible initial and final states in reactions, and n_i is the number density of i -particle, respectively. The Hubble expansion rate in the radiation-dominated era is denoted by H . Note that the decay $h \rightarrow \phi\phi$ is omitted in Eq.(18c) because its decay rate is further suppressed by $g_{B-L}^2 m_h^2 / m_{Z'}^2$, than that of $\phi \rightarrow f\bar{f}$ for small g_{B-L} and α .

Thermally averaged product of the scattering cross section and relative velocity $\langle\sigma v\rangle$ in the right hand side of Eqs. (18) are defined by [36]

$$\langle\sigma v\rangle n_i n_j = \frac{T}{32\pi^4} \sum_{i,j} \int_{(m_i+m_j)^2}^{\infty} ds g_i g_j p_{ij} 4E_i E_j \sigma v K_1 \left(\frac{\sqrt{s}}{T} \right), \quad (19)$$

and

$$\begin{aligned} 4E_i E_j \sigma v &\equiv \prod_f \int \frac{d^3 p_f}{(2\pi)^3} \frac{1}{2E_f} |\mathcal{M}|^2 (2\pi)^4 \delta^{(4)}(p_i + p_j - \sum p_f) \\ &= \frac{1}{16\pi} \frac{2|q_f|}{\sqrt{s}} \int |\mathcal{M}|^2 d\cos\theta, \end{aligned} \quad (20)$$

$$2|q_f| = \sqrt{s - 4m_N^2}, \quad (21)$$

$$p_{ij} \equiv \frac{\sqrt{s - (m_i + m_j)^2} \sqrt{s - (m_i - m_j)^2}}{2\sqrt{s}}. \quad (22)$$

Here, i denotes an initial state with the mass m_i , energy E_i , and internal degrees of freedom g_i . The center-of-mass energy squared is given by $s = (E_i + E_j)^2$, and three-momentum of a final-state particle is denoted by q_f . $K_i(z)$ is the modified Bessel function of the i th kind. For the production processes of Z' with a photon γ , the thermal average of $\sigma v n$ is defined by

$$\langle\sigma v n_i\rangle n_{Z'}^{\text{eq}} \equiv \frac{T}{32\pi^4} \int_{(m_i+m_{Z'})^2}^{\infty} ds g_i g_{Z'} p_{iZ'} (4E_i E_{Z'} \sigma v) K_1 \left(\frac{\sqrt{s}}{T} \right), \quad (23)$$

where $i = \gamma, f, \bar{f}$ and

$$n_{Z'}^{\text{eq}} = \frac{T}{2\pi^2} g_{Z'} m_{Z'}^2 K_2 \left(\frac{m_{Z'}}{T} \right). \quad (24)$$

Thermally averaged decay rate $\langle\Gamma\rangle$ of $i \rightarrow jj$ is defined by

$$\langle\Gamma(i \rightarrow jj)\rangle = \frac{K_1 \left(\frac{m_i}{T} \right)}{K_2 \left(\frac{m_i}{T} \right)} \Gamma(i \rightarrow jj). \quad (25)$$

The ratio of the modified Bessel function represents a suppression factor for a high temperature, $T \gg m_i$, by the time dilation. Concrete forms of the invariant squared amplitudes and

decay rates for the processes involving only N and Z' are given at Appendix in Ref. [34]. The amplitudes for $ij \rightarrow \phi\phi$ are given in Appendix. It should be noted that the productions of N , Z' and ϕ from the decays of particles are treated properly in the thermal averaged cross sections to avoid double-counting in Eqs. (18).

IV. ABUNDANCE OF STERILE NEUTRINO DM

In this section, we show our numerical results of the sterile neutrino DM abundance. Throughout this section, the DM mass m_N and the other sterile neutrino mass m_{ν_R} are fixed to be $m_N = 0.5$ GeV and $m_{\nu_R} = 2$ GeV, respectively, unless stated. We consider the case where Z' cannot decay into a DM pair, hence the Z' mass is restricted to $m_{Z'} \leq 1$ GeV. There are two cases of mass spectrum on $m_\phi > 2m_N$ and $m_\phi < 2m_N$. We consider those in order.

A. $m_\phi > 2m_N$ case

In this spectrum, the DM is produced from the decay $\phi \rightarrow NN$. Figure 1 shows the contour plot of the DM abundance in $m_{Z'}-g_{B-L}$ plane. The blue, red, and green curves correspond to $m_\phi = 100, 20,$ and 2 GeV, respectively. The scalar mixing angle is taken to be $\alpha = 0$ (solid) and 10^{-7} (dashed). The dashed-dotted line corresponds to the lifetime of Z' ; $\tau_{Z'} = 1$ second. The black shaded region is excluded by SN1987A [37]. The gauge coupling constant to reproduce the correct DM abundance turns out to be much smaller than the previous results [34] where the dominant production modes have been regarded as the scattering $Z'Z' \rightarrow NN$, of $t(u)$ -channel N exchange and s -channel scalar h and ϕ exchange, from thermalized Z' initial states. However, what we found here are as follows. If Z' were thermalized, ϕ could be also easily produced by the inverse decay $Z'Z' \rightarrow \phi$, the following decay $\phi \rightarrow NN$ overproduces the DM N . The main production modes of ϕ are the inverse decay $Z'Z' \rightarrow \phi$ and $f\bar{f} \rightarrow \phi$. To suppress the ϕ production by the inverse decay $Z'Z' \rightarrow \phi$ and the Z' production by the scattering $f\gamma \rightarrow fZ'$, whose interaction rates are both proportional to g_{B-L}^2 , we find that g_{B-L} has to be very small. The contours show that $\alpha = 10^{-7}$ cases need further smaller g_{B-L} than $\alpha = 0$ cases because the channel $f\bar{f} \rightarrow \phi$ produces ϕ additionally. We will show this in Figure 3. The solid green line corresponding

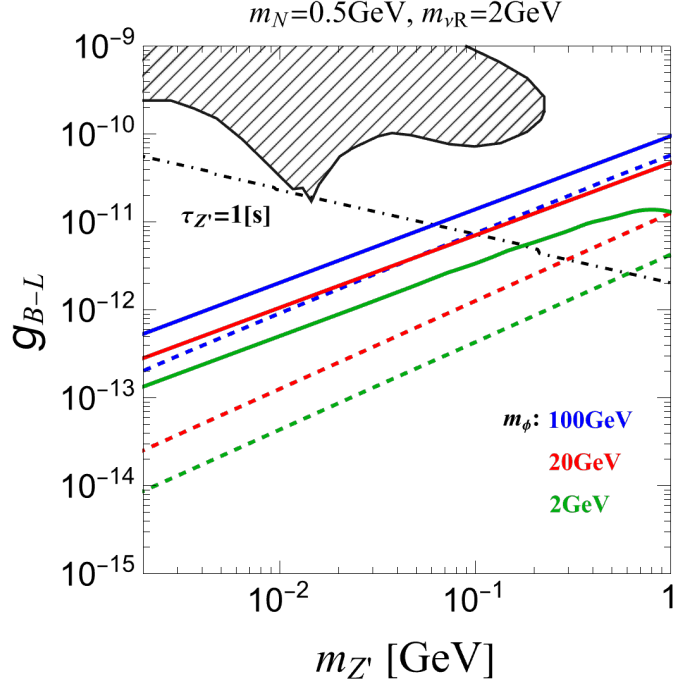


FIG. 1: Contour plots of $\Omega h^2 = 0.12$. The DM mass and the heavier sterile neutrino masses are fixed to $m_N = 0.5$ GeV and 2 GeV, respectively. The blue, red, and green curves correspond to $m_\phi = 100$ GeV, 20 GeV, and 2 GeV, respectively. The scalar mixing angle is taken to $\alpha = 0$ (solid) and 10^{-7} (dashed). The dashed-dotted line represents $\tau_{Z'} = 1$ second. The black shaded region is excluded by SN1987A.

to $\alpha = 0$ and $m_\phi = 2$ GeV deviates from the straight line in the region where $m_{Z'}$ is heavy. This is because $\phi \rightarrow Z'Z'$ approaches its threshold ($m_\phi \simeq 2m_{Z'}$) and the branching fraction becomes smaller. As a result, the branching ratio of $\phi \rightarrow NN$ becomes relatively large and more N is produced. To avoid overproduction, the gauge coupling must be smaller.

Apart from the DM production, the late time decay of Z' into the SM fermions could cause problems. When Z' decays after the Big-Bang nucleosynthesis (BBN), the synthesized elements would be destructed by energetic particles produced by the decay and the success of BBN would be spoiled, as TeV mass gravitinos do [24, 38]. The BBN constraints on sub-GeV decaying particles have been derived in Ref. [39]. For reference purpose, we add the dashed-dotted line representing the Z' lifetime of 1 second in Fig. 1 and below the line the Z' boson would decay after the BBN starts. However, notice that this does not necessarily mean the region below this line is excluded by the BBN. As we will see in Figs. 2 and 3, Z' also can be converted into photon via $Z'f \rightarrow \gamma f$ before its decay. Therefore, the detailed

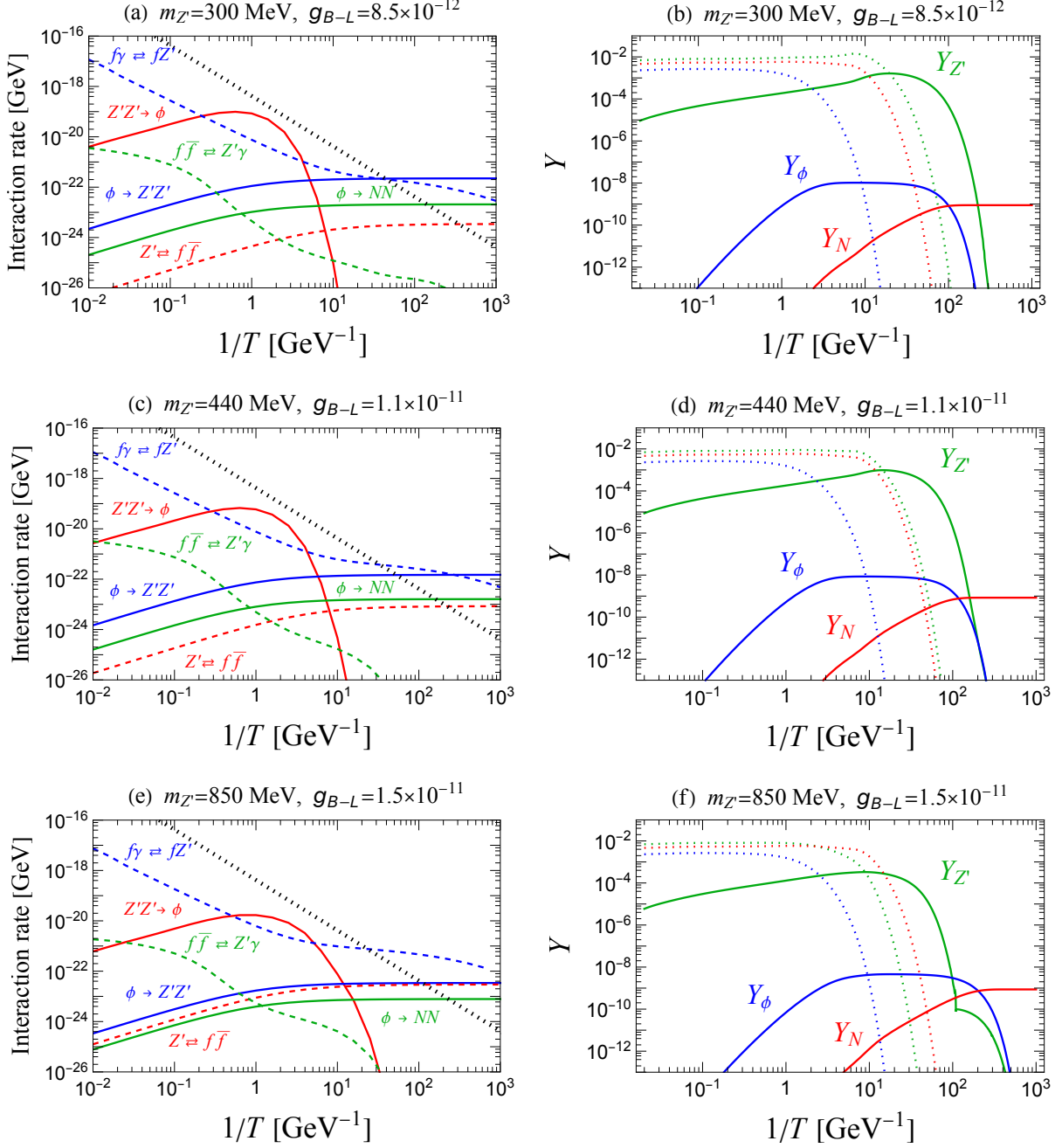


FIG. 2: Time evolution of interaction rates (left) and yield (right). In all panels, the mass of ϕ and scalar mixing angle are fixed as $m_\phi = 2$ GeV and $\alpha = 0$, respectively. In the right panels, the dotted lines represent the time evolution assuming that each particle is in thermal equilibrium.

analysis would be needed by taking into account the conversion into photon.

Figures 2 and 3 show the time evolution of interaction rate $\langle\sigma v(ij \rightarrow kl)\rangle_s$ and $\langle\Gamma(i \rightarrow jk)\rangle$ (panel (a), (c) and (e)), and the yield value Y of N , Z' and ϕ ((b), (d) and (f)) for benchmark points that satisfy $\Omega h^2 = 0.12$. Here, s is the entropy density. The black dotted

line represents the Hubble parameter in the radiation dominated Universe, $H \simeq T^2/M_{pl}$ with the Planck mass $M_{pl} = 2.4 \times 10^{18}$ GeV. In Figure 2, the scalar mass and mixing angle are fixed to be $m_\phi = 2$ GeV and $\alpha = 0$, respectively. The values of $m_{Z'}$ and g_{B-L} are varied in each row: the first, second, and third row of figures correspond to the case $(m_{Z'}, g_{B-L}) = (300 \text{ MeV}, 8.5 \times 10^{-12})$, $(440 \text{ MeV}, 1.1 \times 10^{-11})$, and $(850 \text{ MeV}, 1.5 \times 10^{-11})$, respectively. In the left panels, solid curves represent the interaction rates of ϕ in which the corresponding processes are indicated near each curve. Dashed ones represent those of Z' . One can understand from the left panels that two new processes studied in this paper are dominant production modes of ϕ and Z' . One is the inverse decay $Z'Z' \rightarrow \phi$ which is much larger than $f\bar{f} \rightarrow \phi$. From the inverse decay, ϕ is efficiently produced and then decays into the dark matters roughly below $T \sim 0.1$ GeV from the ϕ decay. The other one is the fermion-photon scattering $f\gamma \rightarrow fZ'$ which can be large in photon bath, which efficiently produces Z' . These Z' can be converted back to photon before it decays. In fact, in the left panels, the interaction rate of the photon scattering $f\gamma \rightarrow fZ'$ is always larger than the decay rate $Z' \rightarrow f\bar{f}$, and becomes comparable to the cosmic expansion rate H before that of the decay rate becomes. Thus, the Z' boson disappears via the conversion rather than the decay in these parameters, which can be seen in the right panels as well. In the right panels in Figs. 2 and 3, solid curves represent the yield of Z' (green), ϕ (blue) and N (red) obtained in our calculation while dashed ones are equilibrium values. One can see that ϕ , Z' and N never enter the thermal bath and are produced in freeze-in mechanism. As explained in the left panels, Z' can be converted into photon by the scattering. Then, $Y_{Z'}$ starts to decrease when the interaction rate of the photon scattering becomes comparable to the Hubble parameter. In panel (f), the behavior of $Y_{Z'}$ evolution changes around $T = 10^{-2}$ GeV. This is because there is still enough ϕ left after $T = 10^{-2}$ GeV, and Z' is produced again through the decay of ϕ .

Figure 3 is the same plot as Figure 2 for $\alpha = 10^{-7}$ (top panels) and 10^{-8} (bottom panels), respectively. Mass parameters are fixed as $m_\phi = 2$ GeV, $m_{Z'} = 100$ MeV. The gauge coupling constant is taken to $g_{B-L} = 4.7 \times 10^{-13}$ (top panels) and 3.3×10^{-12} (bottom panels). In these cases, ϕ can interact with the SM fermions through the scalar mixing. Left panels show that ϕ is produced through not only $Z'Z' \rightarrow \phi$ but also $f\bar{f} \rightarrow \phi$ (solid magenta curve). Due to this new process, ϕ production continues at low temperature after $Z'Z' \rightarrow \phi$ terminates, resulting more ϕ than in $\alpha = 0$ cases. Since the DM is produced from

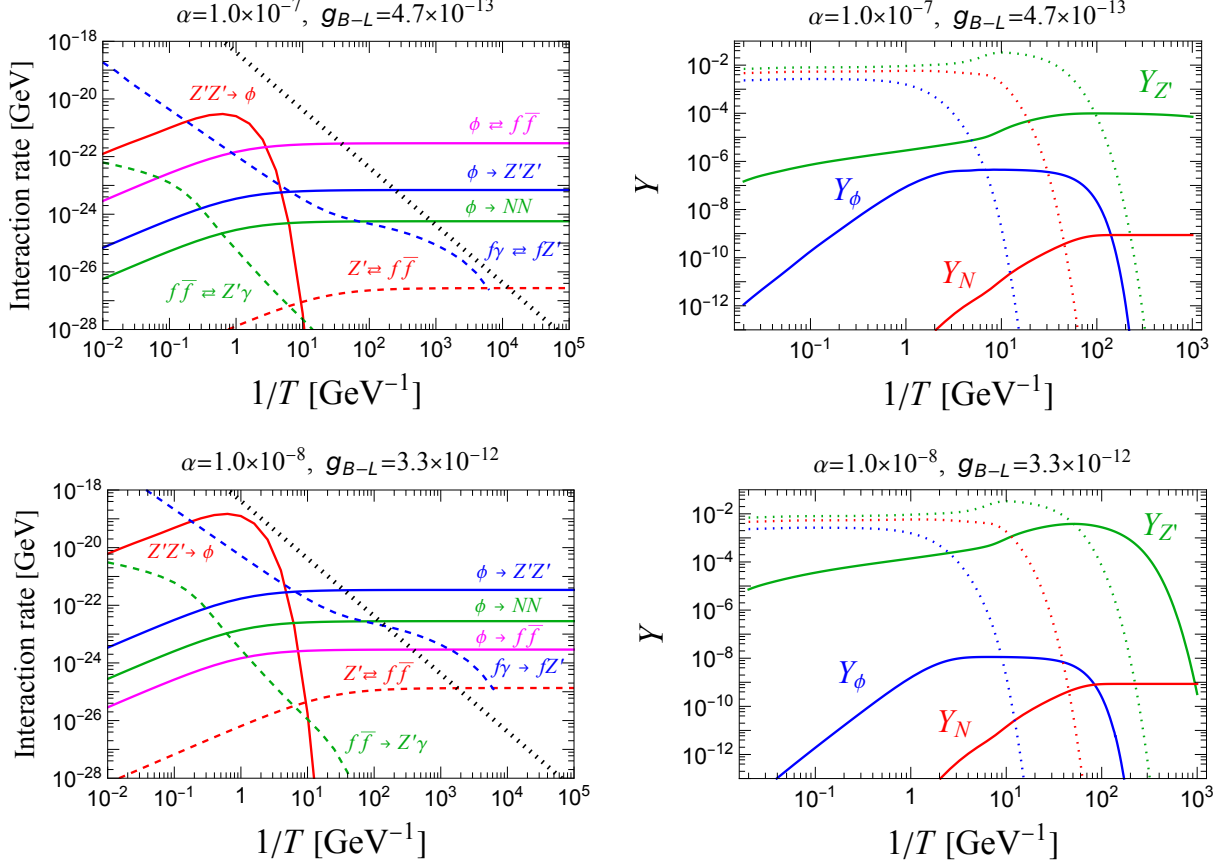


FIG. 3: Plots as figure 2 for $(\alpha, g_{B-L}) = (10^{-7}, 4.7 \times 10^{-13})$ at top row and $(10^{-8}, 3.3 \times 10^{-12})$ at bottom row, respectively. The parameters are taken as $m_\phi = 2$ GeV, $m_{Z'} = 100$ MeV.

the ϕ decay, the gauge coupling should become smaller to suppress the branching ratio into NN as shown in Fig. 1. In the top left panel in Fig. 3, the interaction rate of the photon scattering $f\gamma \rightarrow fZ'$ never become comparable to the expansion rate H and the decay rate becomes so later. Thus, Z' decays during the BBN at $T \simeq 0.1$ MeV. On the other hand, in the bottom panels, Z' can convert into the photon and disappear before the BBN.

B. $m_\phi < 2m_N$ case

Figure 4 is the same plot as Fig. 1 for the mass spectrum $(m_\phi, m_N) = (1 \text{ GeV}, 0.5 \text{ GeV})$ (blue) and $(10 \text{ GeV}, 5 \text{ GeV})$ (red). The brown shaded region is excluded by electron and proton beam dump experiments (See Refs. [35, 40] and references therein). For this mass spectrum, ϕ cannot decay into N and therefore the DM must be produced through the scattering of $Z'Z' \rightarrow NN$, dominantly $t(u)$ -channel N exchange. Hence the results is

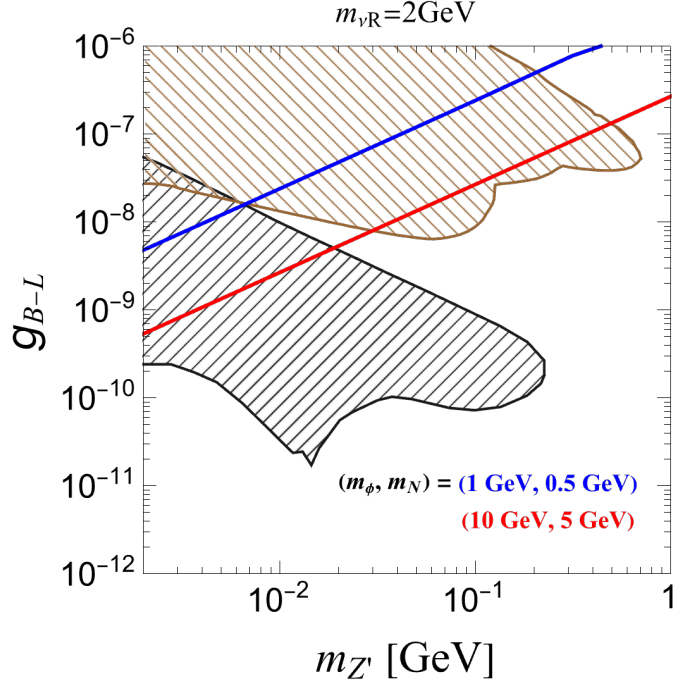


FIG. 4: Blue and red contour plots of $\Omega h^2 = 0.12$ for $(m_\phi, m_N) = (1 \text{ GeV}, 0.5 \text{ GeV})$ and $(10 \text{ GeV}, 5 \text{ GeV})$, respectively. The other sterile neutrino mass m_{ν_R} is taken to be 2 GeV. The black shaded region is excluded by SN1987A. The brown shaded region is excluded by electron and proton beam dump experiments.

insensitive to the scalar mixing α and essentially same as the case B in Ref. [34]. In this case, the Z' boson search will be possible at future FASER experiment [35, 40, 41].

V. CONCLUSION

We have studied freeze-in production of sterile neutrino dark matter in feebly interacting $B-L$ model. In the spectrum where Z' cannot decay into the dark matter, the scalar plays an important role in the dark matter production. We solved the Boltzmann equations of Z' , N and also ϕ simultaneously and analyzed the scalar contribution to the dark matter production. We also took the Z' production with a photon into account.

We found that Z' can be predominantly produced by $f\gamma \rightarrow fZ'$ and produces ϕ through the inverse decay of $Z'Z' \rightarrow \phi$. Then, the sterile neutrino DM is produced by the decay of ϕ . Due to the large number of photon in thermal plasma, the gauge coupling g_{B-L} must be as small as 10^{-13} – 10^{-11} . We showed that not only the DM but also Z' and ϕ never enter

the thermal bath and are produced in freeze-in mechanism. When the scalar mixing α is nonzero, ϕ also is additionally produced by the inverse decays of the SM fermions. Thus, smaller gauge coupling than the one for $\alpha = 0$ case is required not to overproduce the sterile neutrino DM. For such a very small g_{B-L} coupling, Z' may be long-lived and subject of the constraints from the BBN. Such long-lived Z' could disappear by the conversion $fZ' \rightarrow f\gamma$ before its decay, then Z' would not affect the BBN. This is also an interesting aspect of this model and way to avoid BBN constraints.

We also found when the ϕ decay into the DM is forbidden, the gauge coupling should be 10^{-7} – 10^{-6} for $m_{Z'} \leq 1$ GeV. Such a region will be searched by collider experiments like FASER [42, 43]. We will show its sensitivity region in our future work.

Acknowledgments

We thank Shintaro Eijima for valuable discussion on the early state of this work. This work is supported, in part, by JSPS KAKENHI Grants No. JP19K03865, No. JP23K03402 (O.S.), and JSPS KAKENHI Grants No. 22K03622 and 23H01189 (T.S.), by National Natural Science Foundation of China Grant No. NSFC-12347112 (Y.U.), and by the Guangdong Major Project of Basic and Applied Basic Research No. 2020B0301030008 (Y.U.).

Appendix A: Amplitude of the scalar production processes

We give explicit formulas of the invariant amplitude squared. The scalar self-couplings are given in [34].

1. $f(p_1)\bar{f}(p_2) \rightarrow \phi(q_1)\phi(q_2)$

$$M = M_s + M_{tu}, \tag{A1}$$

where

$$M_s = \frac{\sqrt{2}m_f}{v} \bar{v}(p_2)u(p_1) \left(\frac{C_{\phi\phi\phi} \sin \alpha}{(p_1 + p_2)^2 - m_\phi^2 + im_\phi\Gamma_\phi} + \frac{C_{h\phi\phi} \cos \alpha}{(p_1 + p_2)^2 - m_\phi^2 + im_\phi\Gamma_\phi} \right), \quad (\text{A2a})$$

$$M_{tu} = -2 \frac{m_f^2}{v^2} \sin^2 \alpha \times \bar{v}(p_2) \left(\frac{(p_1 - q_1) + m_f}{(p_1 - q_1)^2 - m_f^2 + im_f\Gamma_f} + \frac{(p_1 - q_2) + m_f}{(p_1 - q_2)^2 - m_f^2 + im_f\Gamma_f} \right) u(p_1), \quad (\text{A2b})$$

and

$$C_{\phi\phi\phi} = 3 \frac{m_\phi^2 (2g_{B-L}v \cos^3 \alpha + m_{Z'} \sin^3 \alpha)}{vm_{Z'}}. \quad (\text{A3})$$

2. $Z'(p_1)Z'(p_2) \rightarrow \phi(q_1)\phi(q_2)$

$$M = M_c + M_s + M_{tu}, \quad (\text{A4})$$

where

$$M_c = 16g_{B-L} \cos^2 \alpha \epsilon^\mu(p_1)\epsilon_\mu(p_2), \quad (\text{A5a})$$

$$M_s = -g_{B-L}m_{Z'}\epsilon^\mu(p_1)\epsilon_\mu(p_2) \times \left(\frac{C_{\phi\phi\phi} \cos \alpha}{(p_1 + p_2)^2 - m_\phi^2 + im_\phi\Gamma_\phi} - \frac{C_{h\phi\phi} \sin \alpha}{(p_1 + p_2)^2 - m_\phi^2 + im_\phi\Gamma_\phi} \right), \quad (\text{A5b})$$

$$M_{tu} = 4g_{B-L}^2 m_{Z'}^2 \cos^2 \alpha \epsilon^\mu(p_1)\epsilon_\mu(p_2) \times \left(\frac{1}{(p_1 - q_1)^2 - m_{Z'}^2 + im_{Z'}\Gamma_{Z'}} + \frac{1}{(p_1 - q_2)^2 - m_{Z'}^2 + im_{Z'}\Gamma_{Z'}} \right). \quad (\text{A5c})$$

-
- [1] S. Dodelson and L. M. Widrow, Phys. Rev. Lett. **72**, 17 (1994), hep-ph/9303287.
[2] A. Dolgov and S. Hansen, Astropart. Phys. **16**, 339 (2002), hep-ph/0009083.
[3] T. Asaka, S. Blanchet, and M. Shaposhnikov, Phys. Lett. B **631**, 151 (2005), hep-ph/0503065.
[4] T. Asaka and M. Shaposhnikov, Phys. Lett. B **620**, 17 (2005), hep-ph/0505013.
[5] M. Drewes et al., JCAP **01**, 025 (2017), 1602.04816.
[6] A. Boyarsky, M. Drewes, T. Lasserre, S. Mertens, and O. Ruchayskiy, Prog. Part. Nucl. Phys. **104**, 1 (2019), 1807.07938.

- [7] P. Minkowski, Phys. Lett. B **67**, 421 (1977).
- [8] T. Yanagida, Conf. Proc. C **7902131**, 95 (1979).
- [9] M. Gell-Mann, P. Ramond, and R. Slansky, Conf. Proc. C **790927**, 315 (1979), 1306.4669.
- [10] R. N. Mohapatra and G. Senjanovic, Phys. Rev. Lett. **44**, 912 (1980).
- [11] A. Boyarsky, A. Neronov, O. Ruchayskiy, and M. Shaposhnikov, Mon. Not. Roy. Astron. Soc. **370**, 213 (2006), astro-ph/0512509.
- [12] A. Boyarsky, A. Neronov, O. Ruchayskiy, M. Shaposhnikov, and I. Tkachev, Phys. Rev. Lett. **97**, 261302 (2006), astro-ph/0603660.
- [13] A. Boyarsky, J. Nevalainen, and O. Ruchayskiy, Astron. Astrophys. **471**, 51 (2007), astro-ph/0610961.
- [14] A. Boyarsky, D. Iakubovskiy, O. Ruchayskiy, and V. Savchenko, Mon. Not. Roy. Astron. Soc. **387**, 1361 (2008), 0709.2301.
- [15] H. Yuksel, J. F. Beacom, and C. R. Watson, Phys. Rev. Lett. **101**, 121301 (2008), 0706.4084.
- [16] X.-D. Shi and G. M. Fuller, Phys. Rev. Lett. **82**, 2832 (1999), astro-ph/9810076.
- [17] O. Seto and Y. Toda, Phys. Rev. D **104**, 063019 (2021), 2104.04381.
- [18] A. Davidson, Phys. Rev. D **20**, 776 (1979).
- [19] R. N. Mohapatra and R. Marshak, Phys. Rev. Lett. **44**, 1316 (1980), [Erratum: Phys.Rev.Lett. **44**, 1643 (1980)].
- [20] R. Marshak and R. N. Mohapatra, Phys. Lett. B **91**, 222 (1980).
- [21] S. Khalil and O. Seto, JCAP **10**, 024 (2008), 0804.0336.
- [22] N. Okada and O. Seto, Phys. Rev. D **82**, 023507 (2010), 1002.2525.
- [23] N. Okada and S. Okada, Phys. Rev. D **93**, 075003 (2016), 1601.07526.
- [24] J. R. Ellis, J. E. Kim, and D. V. Nanopoulos, Phys. Lett. B **145**, 181 (1984).
- [25] J. McDonald, Phys. Rev. Lett. **88**, 091304 (2002), hep-ph/0106249.
- [26] L. J. Hall, K. Jedamzik, J. March-Russell, and S. M. West, JHEP **03**, 080 (2010), 0911.1120.
- [27] K. Kaneta, Z. Kang, and H.-S. Lee, JHEP **02**, 031 (2017), 1606.09317.
- [28] A. Biswas and A. Gupta, JCAP **09**, 044 (2016), [Addendum: JCAP **05**, A01 (2017)], 1607.01469.
- [29] S. Heeba and F. Kahlhoefer, Phys. Rev. D **101**, 035043 (2020), 1908.09834.
- [30] O. Seto and T. Shimomura, Phys. Lett. B **811**, 135880 (2020), 2007.14605.
- [31] N. Okada, S. Okada, and Q. Shafi, Phys. Lett. B **810**, 135845 (2020), 2003.02667.

- [32] H. Okada, Y. Orikasa, and Y. Shoji, *JCAP* **07**, 006 (2021), 2102.10944.
- [33] S. Iwamoto, K. Seller, and Z. Trócsányi, *JCAP* **01**, 035 (2022), 2104.11248.
- [34] S. Eijima, O. Seto, and T. Shimomura, *Phys. Rev. D* **106**, 103513 (2022), 2207.01775.
- [35] K. Asai, A. Das, J. Li, T. Nomura, and O. Seto, *Phys. Rev. D* **106**, 095033 (2022), 2206.12676.
- [36] P. Gondolo and G. Gelmini, *Nucl. Phys. B* **360**, 145 (1991).
- [37] D. Croon, G. Elor, R. K. Leane, and S. D. McDermott, *JHEP* **01**, 107 (2021), 2006.13942.
- [38] M. Y. Khlopov and A. D. Linde, *Phys. Lett. B* **138**, 265 (1984).
- [39] M. Kawasaki, K. Kohri, T. Moroi, K. Murai, and H. Murayama, *JCAP* **12**, 048 (2020), 2006.14803.
- [40] J. L. Feng et al., *J. Phys. G* **50**, 030501 (2023), 2203.05090.
- [41] T. Araki, K. Asai, H. Otono, T. Shimomura, and Y. Takubo, *JHEP* **03**, 072 (2021), [Erratum: *JHEP* **06**, 087 (2021)], 2008.12765.
- [42] A. Ariga et al. (FASER), *Phys. Rev. D* **99**, 095011 (2019), 1811.12522.
- [43] H. Abreu et al. (FASER), *Phys. Lett. B* **848**, 138378 (2024), 2308.05587.